analytical chemistry

Article

pubs.acs.org/ac

Structural Analysis of Low Molecular Weight Heparin by Ultraperformance Size Exclusion Chromatography/Time of Flight Mass Spectrometry and Capillary Zone Electrophoresis

Qianqian Zhang,[†] Xi Chen,[‡] Zhijia Zhu,[§] Xueqiang Zhan,[§] Yanfang Wu,[§] Lankun Song,[‡] and Jingwu Kang*[,†]

[†]Shanghai Institute of Organic Chemistry, Chinese Academy of Sciences, Lingling Road 345, Shanghai 200032, China

[‡]Waters Corporation, Block 13, Jinhai Road 1000 , Pudong New District, Shanghai 201206, China

[§]College of Chemistry, Chemical Engineering and Biotechnology, Donghua University, Shanghai 201620, China

Supporting Information

ABSTRACT: Although low molecular weight heparins (LMWHs) have been used as anticoagulant agents for over 2 decades, their structures have not been fully characterized. In this work, we propose a new strategy for the comprehensive structural analysis of LMWHs based on the combination of ultraperformance size exclusion chromatography/electrospray quadruple time-of-flight-mass spectrometry (UPSEC/Q-TOF-MS) and capillary zone electrophoresis (CZE). More than 70 components, including oligosaccharides with special structures such as 1,6-anhydro rings, saturated uronic acid at the nonreducing end and odd-numbered saccharides units were identified with UPSEC/Q-TOF-MS. Furthermore, a more detailed compositional analysis was accomplished by CZE analysis. PEG10000 and $MgCl_2$ were added to the background electrolyte to separate those saccharides with the nearly same charge-to-mass ratio. Baseline separation and quantification of all the building blocks of the most complex LMWH, namely, enoxaparin, which include 10 disaccharides, 1 trisaccharide, 2 tetrasaccharides, and, of particular importance, 4 1,6-anhyro derivatives, was achieved using CZE for the first time. Additionally, the peaks of oligosaccharides, in the absence of commercially available standards, were assigned on the basis of the linear correlation between the electrophoretic mobilities of oligosaccharides and their charge-to-mass ratios. These two approaches are simple and robust for structural analysis of LMWHs.

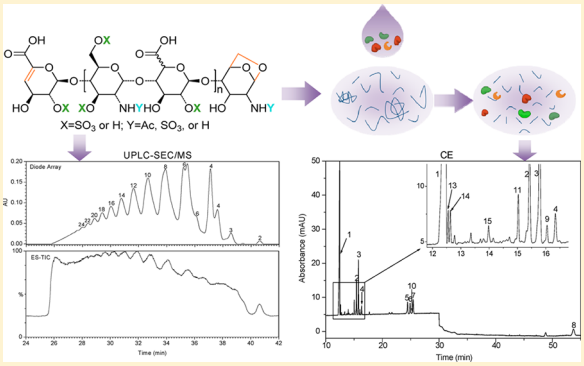

Low molecular weight heparins (LMWHs) have been used for the treatment and prophylaxis of thromboembolism for over 2 decades with the advantages of less bleeding, greater bioavailability, and more predictable anticoagulant effects in comparison with unfractionated heparins (UFHs).[1,2] Recently, additional potential pharmaceutical applications of LMWHs for diseases such as cancer,[3] diabetes,[4] and senile dementia[5] have also been reported. However, their structure−function relationship has not been fully understood due to their high structural complexity.[6] LWMHs, which are derived from UFHs by enzymatic or chemical depolymerization, inherit the repeating disaccharide units composed of a glucosamine residue and an uronic acid residue (iduronic or glucuronic acid).[7−9] The various sulfation patterns, acetylation modifications, epimerization of glucoronic acid to iduronic acid, and various chain lengths lead to considerable heterogeneity.[10] In addition, with an average of 2.7 sulfate residues per disaccharide unit, heparin has the highest negative charge density of any known biological macromolecule. Compared to UFHs, LMWHs are more complicated in composition and sequence because of the structural alterations induced by harsh enzymatic or chemical manufacturing procedures. These alterations give rise to the different biochemical and pharmacological properties that are observed in various LMWHs.[11] For example, enoxaparin, the most commonly used LMWH,[6,12] is produced by the alkaline degradation of UFHs through β-eliminative cleavage. Most of the oligosaccharide chains in enoxaparin possess 4,5-unsaturated uronic acid residues at the nonreducing end, and some have a 1,6-anhydro ring structure at the reducing end, which is considered to be the characteristic structure of enoxaparin.[11] Recently, it has been reported that oligosaccharides of heparin containing 1,6-anhydro rings exhibited weaker binding to antithrombin III than those without 1,6-anhydro rings.[13] Additionally, 1,6-anhydro rings have been associated with the release of tissue factor pathway inhibitor, the inhibition of the contact-kinin system, and the proliferation of smooth muscle and endothelial cells.[14] Because the 1,6-anhydro ring is closely related to the biological activity of enoxaparin, the European

Received: November 1, 2012
Accepted: December 28, 2012

dx.doi.org/10.1021/ac303185w | *Anal. Chem.* XXXX, XXX, XXX−XXX

Medicines Agency (EMA) and the U.S. Food and Drug Administration (FDA) require that the molar percentage of oligosaccharide chains containing 1,6-anhydro rings in enoxaparin should fall in the range of 15−25%. Moreover, minor structural variations of LMWHs between different lots or different manufacturers can also influence their pharmacokinetics and pharmacodynamics. Therefore, structural analysis is the starting point for a deeper understanding of the structure−function relationship of LMWHs.[15]

The most common strategy used for the structural analysis of LMWHs is the bottom-up approach. In this approach, LWMHs are first depolymerized into disaccharide building blocks via exhaustive enzymatic digestion with a mixture of heparinases (I, II, and III), and the resulting mixture is quantitatively analyzed with various separation techniques such as strong anion exchange chromatography (SAX), reversed phase ion pair chromatography (RPIP), and capillary electrophoresis (CE).[15−20] Recently, mass spectrometry (MS) coupling with RPIP[21−25] have been also used for disaccharide compositional analysis. However, thus far, SAX high performance liquid chromatography (HPLC) is the only method used for the quantitative analysis of the 1,6-anhydro derivatives.[26] The disadvantage of this method is that the SAX-column is easily contaminated by bovine serum albumin and heparinases present in the digestion buffer. Therefore, there is an urgent need to develop a better method for this purpose.

Another strategy used for the structural analysis of LMWHs is the top-down approach, in which the intact oligosaccharide chains can be directly analyzed without prior digestion with enzymes. Thus far, it remains a difficult task to directly characterize all components of LMWHs due to their high complexity and the lack of authentic standards.[21,26] Although NMR plays a key role in the structural elucidation of oligosaccharides,[27] the requirement of a large amount of pure sample hinders the application of this technique. Alternatively, mass spectrometry (MS) is an increasingly promising technique for the analysis of LMWHs owing to its advantages of high sensitivity and ability to provide abundant structural information.[28−32] Coupling MS with separation techniques greatly enhances its capacity for structural analysis of intact LWMHs. Several methods including size exclusion chromatography (SEC)/MS,[33] RPIP/LC/MS,[34,35] and HILIC/Chip-LC/MS[36] have been developed for this purpose. Most recently, Linhardt et al.[37] utilized HILIC/Fourier transform mass spectrometry (FTMS) for the direct characterization of intact LMWH. Heparin oligosaccharides can be quantitatively analyzed without special sample preparation.

Compared to other separation techniques, SEC displays several advantages, such as simple and robust separation mechanism, compatibility with electrospray ionization (ESI)-MS analysis, and effective profiling of the components.[38−40] Moreover, its capacity of online desalting can reduce the formation of alkali metal adducts which cause spectral complexity and decreased sensitivity.[38] Most recently, an ultraperformance SEC (UPSEC) column packed with 1.7 μm particles has been developed. Compared with conventional SEC columns, the UPSEC column provides much greater separation efficiency and resolution which may be helpful to get more detailed structural information.

Herein, we described a new strategy used for the comprehensive characterization of enoxaparin, one of the most complex LMWHs, using ultraperformance size exclusion chromatography/electrospray quadruple time-of-flight-mass spectrometry (UPSEC/Q-TOF-MS) combined with capillary zone electrophoresis (CZE). With the high resolution of UPSEC/Q-TOF-MS, more than 70 components in enoxaparin, including those oligosaccharides with saturated uronic acid or the 1,6-anhydro ring as well as trisaccharides were identified; furthermore, almost all the building blocks of LMWHs including 1,6-anhydro derivations were separated and quantitated with CZE. CE has been demonstrated to be a powerful method for the separation of heparin sulfated oligosaccharides due to its high separation efficiency.[18−20] However, to the best of our knowledge, this is the first report of the utilization of CE to detect and measure the molar percentage of 1,6-anhydro derivatives. Compared with the original SAX-HPLC method, the new CZE method is simpler, faster, and more cost-effective.

EXPERIMENTAL SECTION

Reagents and Chemicals. Heparinases I, II, III from *Flavobacterium heparinum* and eight heparin disaccharide standards, namely, ΔIS, ΔIIS, ΔIIIS, ΔIVS, ΔIA, ΔIIA, ΔIIIA, and ΔIVA, were purchased from Iduron (Manchester, U.K.). The reference standard for enoxaparin sodium was purchased from United States Pharmacopeia (USP, Rockville, MD). Two other lots of enoxaparin sodium were obtained from two different manufacturers. Tris(hydroxymethyl)-aminomethane and ammonium acetate (TEA) were purchased from Sigma-Aldrich (St. Louis, MO). Phosphoric acid, calcium acetate, sodium hydroxide, and acetic acid were obtained from Shanghai Fourth Chemical Reagent (Kunshan, Jiangsu, China). Water and methanol (MeOH) were of LC/MS grade available from Fisher Scientific (Fair Lawn, NJ).

The CE background electrolyte consisted of 200 mM Tris-H_3PO_4 buffer containing 1.25% (w/v) PEG10000 and 2.5 mM $MgCl_2$ adjusted to pH 2.5 with 1 M H_3PO_4. Sodium/calcium acetate buffer was prepared with 2 mM calcium acetate and 0.1 mg/mL BSA, and the pH was adjusted to 7.0 with 2 M NaOH. All solutions of heparin and LMWHs were prepared at a concentration of 20 mg/mL. The stock solutions of disaccharide standards ΔIS, ΔIIIS, ΔIA, ΔIIS, ΔIVA, ΔIVS, ΔIIA, and ΔIIIA were prepared at a concentration of 0.25 mg/mL. Heparinases I, II, and III were dissolved in 10 mM KH_2PO_4 buffer (pH 7.0) containing 0.2 mg/mL BSA to give an activity of 0.133 IU/mL for each enzyme. The heparinase mixture was stored at −20 °C prior to use. All solutions were prepared in ultrapure water (18 MΩ cm) purified by a Milli-Q water purifier (Millipore Corporation, Milford, MA). The solutions were filtered through a 0.45 μm membrane filter prior to use.

Exhaustive Enzymatic Digestion of LMWHs. LMWHs in solution (20 μL), sodium/calcium acetate buffer (70 μL), and heparinase cocktail (100 μL) were combined, gently mixed, and incubated for at least 48 h in a 25 °C water bath. The depolymerized solution was directly injected into the capillary to perform electrophoresis. For SAX-HPLC analysis, the completely depolymerized sample solution was reduced using sodium borohydride prior to injection.

Ultraperformance Size Exclusion Chromatography. SEC separations were performed on an Acquity UPLC system (Waters Corporation, Milford, MA) equipped with a photodiode array (PDA) detector monitored at 232 nm. The LMWHs were separated on tandem Acquity UPLC BEH 125 SEC columns (4.6 mm × 150 mm and 4.6 mm × 300 mm, Waters, Milford, MA) packed with 1.7 μm particles. The column temperature was maintained at 25 °C, and the flow rate

dx.doi.org/10.1021/ac303185w | Anal. Chem. XXXX, XXX, XXX−XXX

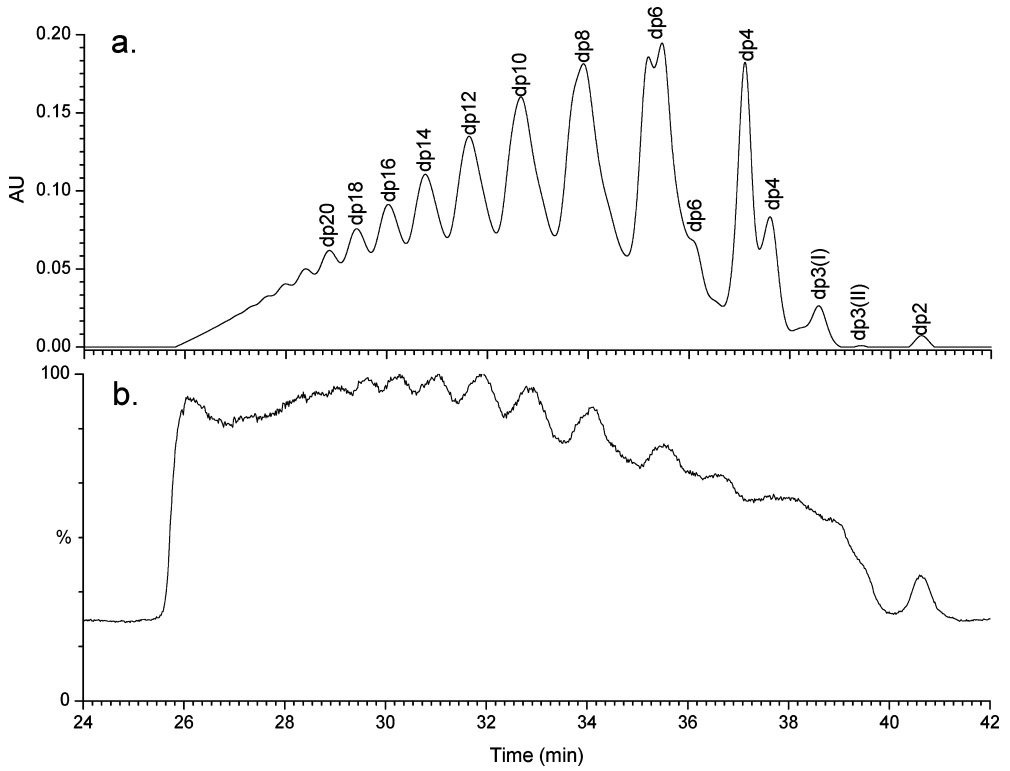

Figure 1. Analysis of enoxaparin sodium by online coupled SEC/MS. (a) UV chromatogram recorded at 232 nm and (b) TIC chromatogram.

was set to 0.1 mL/min. The injection volume was 5 μL. Eluent A was 50 mM ammonium acetate without pH adjustment, and Eluent B was MeOH. Isocratic elution was implemented by maintaining eluent B at 20%. Total elution time was 50 min.

Mass Spectrometry. The Acquity UPLC system was coupled to a hybrid quadruple time-of-flight mass spectrometer, a SYNAPT G2 HDMS system (Waters Corporation, Milford, MA) with a standard ESI source. The data acquisition and analysis were performed with Masslynx 4.1 software. The instrument was operated in negative mode with a capillary voltage of 2.5 kV, a source temperature of 120 °C, and a desolvation temperature of 400 °C. The sampling cone voltage was set at 10 V, and the extraction cone was set to 4 V to minimize in-source fragmentation induced by loss of sulfates in heparin.

Capillary Zone Electrophoresis. All CZE separations were performed on an Agilent CE system equipped with a DAD detector (Waldbronn, Germany). Data were processed using the Agilent CE ChemStation Software. A fused-silica capillary with 50 μm i.d. (370 μm o.d.) × 80 cm (effective length 71.5 cm from the inlet to the detection window) was purchased from Polymicro Technologies (Phoenix, AZ). The capillary was thermostatted at 25 °C. All analytes were detected by UV absorbance at 232 nm. The new capillary was pretreated with 1 M NaOH solution for 30 min, followed by flushing with deionized water and running buffer for 5 min each. Prior to each run, the capillary was rinsed for 3 min each with 1 M NaOH, deionized water, and the running buffer. Samples were loaded by pressure injection at 50 mbar for 15 s. The separations were performed by applying a voltage of −25 kV. During the electrophoresis process, a pressure of 20 mbar was applied at 28 min to pass the unsulfated disaccharide ΔIVA through the detection window.

Strong Anion Exchange High performance Liquid Chromatography. An Agilent 1260 liquid chromatography system (Agilent Technologies, Germany) with a UV detector monitored at 232 nm was employed. Enoxaparin-derived disaccharides were separated on a Phenomenex SAX column (4.6 mm × 150 mm) with a guard column. The injection volume was 10 μL. The column was eluted at a flow rate of 0.65 mL/min and maintained at 50 °C. Gradient elution was performed using a binary solvent system. Eluent A was 2.3 mM NaH_2PO_4 at pH 3.0, and eluent B was 2 M $NaClO_4$ and 2.3 mM NaH_2PO_4 at pH 3.0. The gradient program was as follows: 3−35% B from 0−20 min, then 35−100% B from 20−50 min.

RESULTS AND DISCUSSION

Structure Profiling of LMWHs with UPSEC/Q-TOF-MS. The optimum SEC separation of LMWHs was achieved using two serially connected UPLC BEH 125 SEC columns (4.6 mm × 150 mm and 4.6 mm × 300 mm, packed with 1.7 μm particles) at a flow rate of 0.1 mL/min. A volatile mobile phase consisting of 50 mM ammonium acetate and 20% (v/v) methanol was amenable to MS detection.

The obtained UV and total ion chromatograms are shown in Figure 1. Compared with conventional SEC,[39] UPSEC offers much higher resolved fractionation of LWMHs. As shown in Figure 1a, the components of an enoxaparin sample were effectively fractionated based on size into more than a dozen fractions up to dp24. However, the mass spectrum for each fraction was still too complex to be completely interpreted, as each fraction contained a mixture of two or more components with various sequences and degrees of sulfation. With increasing degrees of polymerization, the LMWH oligosaccharides became multiply charged, further complicating the spectra. Therefore, deconvolution of the raw mass data was necessary to simplify the MS analysis. In the deconvoluted mass spectra, the

dx.doi.org/10.1021/ac303185w | Anal. Chem. XXXX, XXX, XXX−XXX

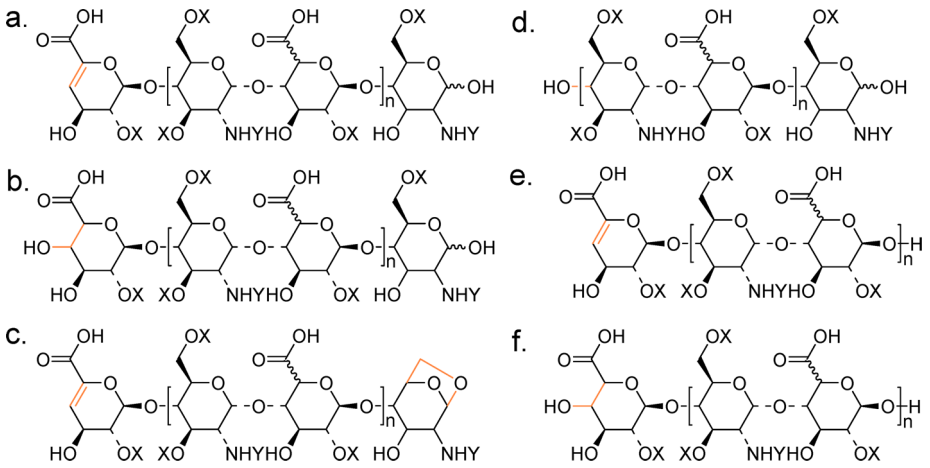

Figure 2. Structures of oligosaccharides found in enoxaparin. (a) Main oligosaccharides with even numbers of units and unsaturated uronic acid at the nonreducing end; (b) oligosaccharides with even numbers of units and saturated uronic acid at the nonreducing end; (c) oligosaccharides with a 1,6-anhydro structure at the reducing end; (d, f) oligosaccharides with odd numbers of units and saturated uronic acid at the nonreducing end; (e) oligosaccharides with odd numbers of units and unsaturated uronic acid at the nonreducing end. X = SO_3 or H, Y = SO_3, Ac, or H.

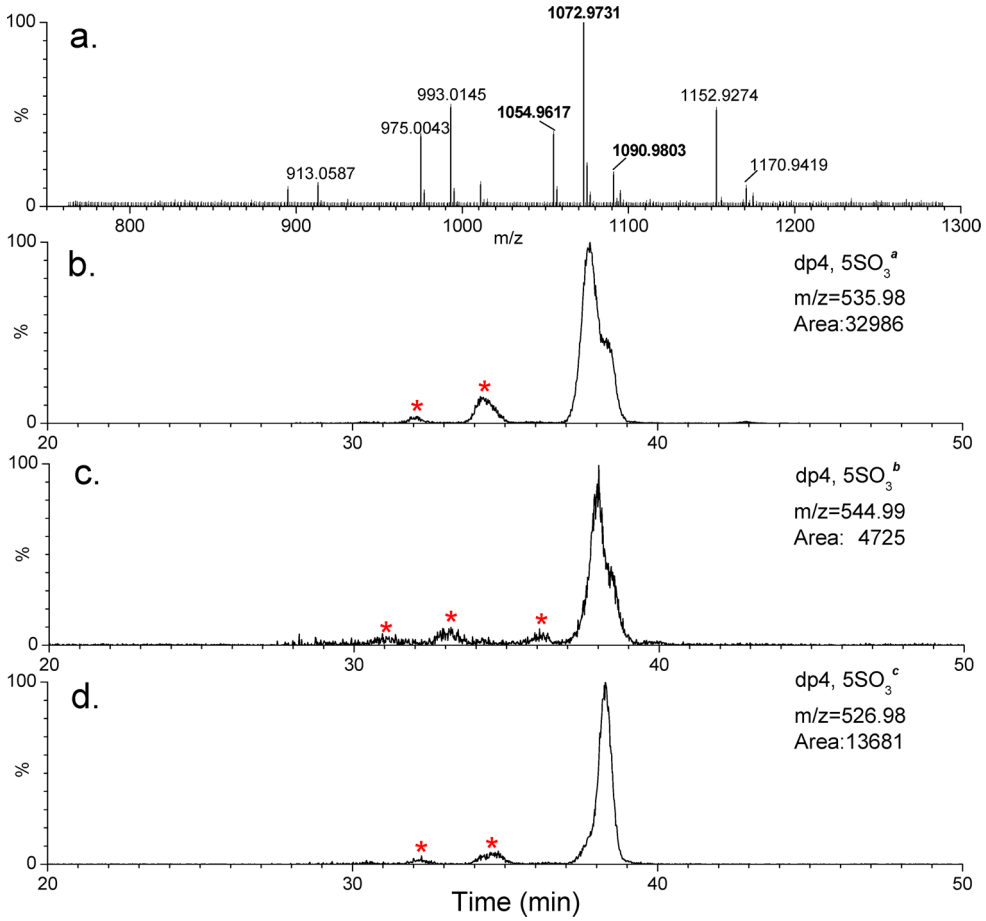

Figure 3. (a) The deconvoluted mass spectra of the tetrasaccharides obtained in the retention time window 37.8−38.0 min. (b) EIC of the tetrasaccharide with the most basic structure (Figure 2a). (c) EIC of the tetrasaccharide with a saturated uronic acid (Figure 2b). (d) EIC of the tetrasaccharide with a 1,6-anhyro structure at the reducing end (Figure 2c). EICs were created by setting the mass chromatogram window at 50 ppm. Peaks labeled with an asterisk represent multiply charged oligosaccharides with a higher dp number.

vast majority of peaks corresponded to single deprotonated molecular ions $[M - H]^-$. Sodium and other cation adducts seldom appeared owing to the effective desalting by UPSEC.[38]

In this experiment, more than 70 components in enoxaparin sodium were identified. The data are presented in the Supporting Information, Table S1. Most of the components could be assigned to one of six categories of general sequence structures, as shown in Figure 2. Spectral interpretation of larger oligosaccharides with degrees of polymerization greater

dx.doi.org/10.1021/ac303185w | Anal. Chem. XXXX, XXX, XXX−XXX

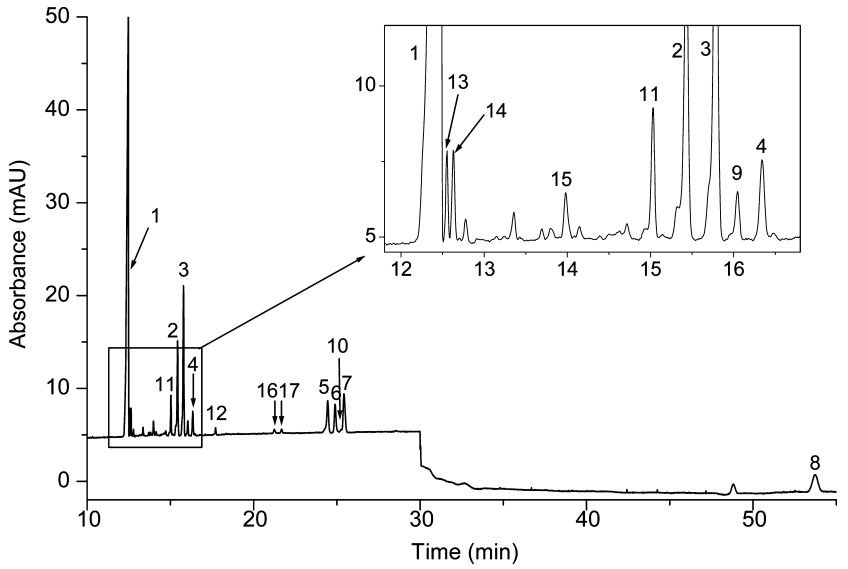

Figure 4. Electropherogram of oligosaccharides derived from exhaustively digested enoxaparin sodium. Conditions: background electrolyte, 200 mM Tris-H_3PO_4 buffer (pH 2.5) containing 2.5 mM $MgCl_2$ and 1.25% PEG; separation voltage, −25 kV; detection wavelength UV232 nm. Peaks: 1 = ΔIS; 2 = ΔIIIS; 3 = ΔIIS; 4 = ΔIA; 5 = ΔIVS; 6 = ΔIIIA; 7 = ΔIIA; 8 = ΔIVA; 9 = ΔIIS_{gal}; 10 = ΔIVS_{gal}; 11= $\Delta IIA\text{-}IIS_{glu}$; 12 = $\Delta IIA\text{-}IVS_{glu}$; 13 = trisaccharide; 14 = 1,6-anhydro ΔIS-IS epi; 15 = 1,6-anhydro ΔIS; 16 = 1,6-anhydro ΔIIS; 17 = 1,6-anhydro ΔIIS epi.

Table 1. Electrophoretic Mobility (μ) for Each Oligosaccharide

peak no.	oligosaccharide	molecular weight	no. of SO_3^- units	q/m (10^{-3})	measured μ_{ep} (10^{-4} cm^2/s V)	calculated μ_{ep} (10^{-4} cm^2/s V)
1	ΔIS	665	3	4.511	3.703	3.696
2	ΔIIIS	563	2	3.552	3.129	3.119
3	ΔIIS	563	2	3.552	3.076	3.119
4	ΔIA	605	2	3.306	2.993	2.971
5	ΔIVS	461	1	2.169	2.243	2.287
6	ΔIIIA	503	1	1.988	2.216	2.178
7	ΔIIA	503	1	1.988	2.185	2.178
8	ΔIVA	401	0	0		
9	ΔIIS_{gal}	563	2	3.552	3.039	3.119
10	ΔIVS_{gal}	461	1	2.169	2.2	2.287
11	ΔIIA-IISglu	1168	4	3.425	3.194	3.042
12	ΔIIA-IVSglu	1066	3	2.814	2.819	2.675
13	trisaccharide	965	4	4.145	3.685	3.475
14	1,6-anhydroΔIS-IS epi	1210	5	4.132	3.665	3.468
15	1,6-anhydro ΔIS	545	2	3.670	3.374	3.190
16/17	1,6-anhydro ΔIIS/ΔIIS epi	443	1	2.257	2.455	2.339

than 18 was difficult due to the overlapping of their isotopic clusters.

Interestingly, besides the most abundant oligosaccharides with terminal unsaturated uronic acid residues, peaks arising from saturated oligosaccharides with an additional 18 Da mass were also observed in the mass spectra for enoxaparin. These oligosaccharides were derived from the original nonreducing ends of the parent heparin chains and could not be monitored via UV detection at 232 nm because they lacked a chromophore. Moreover, the peaks arising from 1,6-anhydro oligosaccharides were also observed with masses 18 Da less than unsaturated oligosaccharides. These species may be semiquantitatively determined. For this purpose, the deconvoluted mass spectrum of tetrasaccharides in the retention time window 37.8−38.0 min was constructed (shown in Figure 3a). The most abundant ion, 1072.9713, was assigned as an unsaturated tetrasaccharide bearing five sulfated groups. The peaks appearing at 18 Da more (1090.9803) and 18 Da less (1054.9617) than the dominant ion were assigned as a saturated tetrasaccharide and 1,6-anhydro tetrasaccharide, respectively. Their extracted ion chromatograms (EIC) were created from the doubly charged ions, which were the most abundant charged molecular ions for these tetrasaccharides (shown in Figure 3b−d). The peak areas of the tetrasaccharides were obtained from the EICs; the peak area ratios among the unsaturated, saturated, and 1,6-anhydro ring tetrasaccharides were calculated as 1:0.14:0.41. This ratio is generally consistent with the values measured by SAX-HPLC and CZE (as discussed below). Therefore, UPSEC/Q-TOF-MS can be used for rapidly scanning for changes in the components of LMWHs, especially during the manufacturing process which is susceptible to a number of factors, e.g., temperature and depolymerization time.

In addition, oligosaccharides with an odd number of monosaccharide units (Figure 2d−f) were also found in enoxaparin. A trisaccharide with a saturated glucosamine at the nonreducing end (Figure 2d) was eluted in SEC and labeled as dp3 (I). Because it lacked a chromophore, it could

dx.doi.org/10.1021/ac303185w | Anal. Chem. XXXX, XXX, XXX−XXX

not be monitored by UV detection but responded to the high ion current in MS (Figure 1). Two other trisaccharides with unsaturated (Figure 2e) and saturated (Figure 2f) uronic acid residues at the nonreducing ends were identified in the fraction labeled as dp3 (II). The longer oligosaccharides with odd numbers of monosaccharide units could not be identified due to their low abundance in enoxaparin and relatively low resolution of SEC.

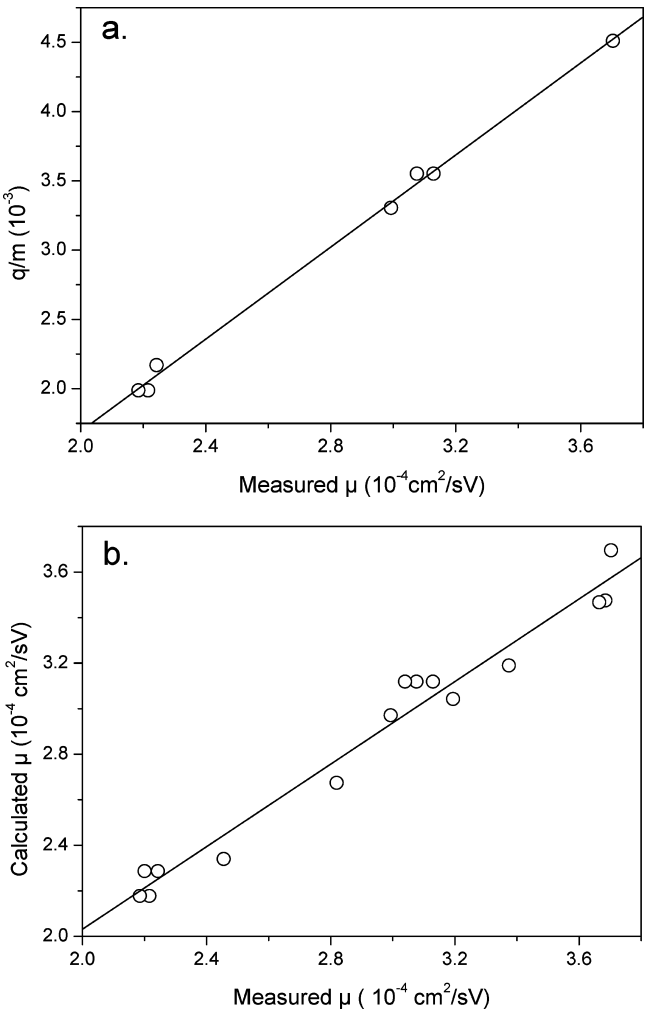

Figure 5. Correlation plots of (a) the measured electrophoretic mobility (μ) of the standard disaccharides (1−7) versus their corresponding net charge-to-mass ratios (q/m), and part b is the calculated mobility versus the measured mobility for all building blocks. Electrophoresis conditions were the same as in Figure 1. Each point was measured in triplicate.

Although SEC/UV/Q-TOF-MS is a rapid and sensitive tool for analyzing long chain oligosaccharides in LMWHs, its application to the quantitative analysis of LMWHs is limited by a lack of reference standards. Therefore, a CZE-based method for the accurate quantitation of all building blocks was developed.

Development of CZE Method. Almost all oligosaccharides derived from exhaustive enzymatic digestion were baseline separated by CZE using an optimal background electrolyte consisting of 200 mM Tris-H_3PO_4 buffer containing 1.25% PEG10000 and 2.5 mM $MgCl_2$ (Figure 4). We found that the addition of both poly(ethylene glycol) (PEG) and $MgCl_2$ to the running buffer was indispensable for resolving the comigrated peaks numbered as 1, 13, and 14 (Figure S1 in the Supporting Information). The effects of the concentration of PEG (0.5−1.5%, w/v) on the separation were investigated by keeping the $MgCl_2$ concentration at 2.5 mM. The resolution increased with increasing PEG concentration up to 1.25% (w/v), while increasing the concentration further produced a noisy baseline. The effect of the $MgCl_2$ concentration on the resolution of peaks 1, 13, and 14 was also investigated by keeping the PEG concentration at 1.25% (w/v). The optimal concentration of $MgCl_2$ was determined to be 2.5 mM. The improved separation upon addition of PEG and $MgCl_2$ to the running buffer was probably due to the sieving effect produced by PEG molecular chains and modification of the electrophoretic mobility by the formation of transient ion pairs between Mg^{2+} and the sulfate groups of the oligosaccharide chains. Additionally, it was found that the buffer pH also played a key role in improving the separation of peaks 1, 13, and 14 (Figure S2 in the Supporting Information). The best separation was achieved at pH 2.5, at which the nonsulfated ΔIVA (pK_a 3.1−3.2) was no longer charged and could not be electrophoretically driven.[9] Therefore, 20 mbar pressure was applied to the inlet of the capillary to pass the ΔIVA (labeled as 8) through the detection window at 28 min when most of the other components had been separated (Figure 4).

Quantitative Compositional Analysis of Exhaustively Digested Enoxaparin with CZE. Under optimal conditions, all possible building blocks of enoxaparin including 10 disaccharides, 1 trisaccharide, 2 tetrasaccharides, and 4 1,6-anhydro derivatives (listed in the Supporting Information, Table S2) were baseline separated. In a typical electropherogram (Figure 4), the peaks belonging to eight elementary disaccharides (numbered 1−8) were identified by individually spiking each standard disaccharide into the exhaustively digested enoxaparin sample. The peak was identified as a given disaccharide if the peak height increased upon addition of that disaccharide to the sample. However, because of the lack of authentic standards, it was impossible to directly assign the peaks belonging to 1,6-anhydro derivatives (1,6-anhydro ΔIS, 1,6-anhydro ΔIIS, 1,6-anhydro ΔIIS epi, and 1,6-anhydro ΔIS-ΔIS) and other oligosaccharides. Therefore, we adopted an indirect approach based on the linear relationship between the electrophoretic mobility and the charge-to-mass ratio of the heparin oligosaccharides.[41]

In our experiment, under the optimal conditions at pH 2.5, μ_{eof} was determined to be 0.762×10^{-4} cm^2/s V with the EOF marker DMSO. The measured μ_{ep} values of the seven standard oligosaccharides are given in Table 1. In addition, according to the Debye−Hükel−Henry theory, at a given pH, the electrophoretic mobility of a charged species depends on the charge-to-mass (radius) ratio.[42,43] At pH 2.5, the sulfo groups (p$K_a \approx$ 0.5−1.5)[44] remained ionized while the carboxyl groups of uronic acid were no longer charged (p$K_a \approx$ 3.5).[41] Therefore, the net charge of each oligosaccharide was approximately equivalent to the number of the associated sulfo groups. Seven standard disaccharides (numbered 1−7 in Table S2 in the Supporting Information) were used to construct a linear relationship between the charge-to-mass ratio and their measured μ_{ep} values (1−7, shown in Figure 5a). The regressed linear equation (R^2 = 0.997) is given below.

$$\frac{q}{m} = 1.662\mu_{ep} - 1.631 \quad (1)$$

dx.doi.org/10.1021/ac303185w | Anal. Chem. XXXX, XXX, XXX−XXX

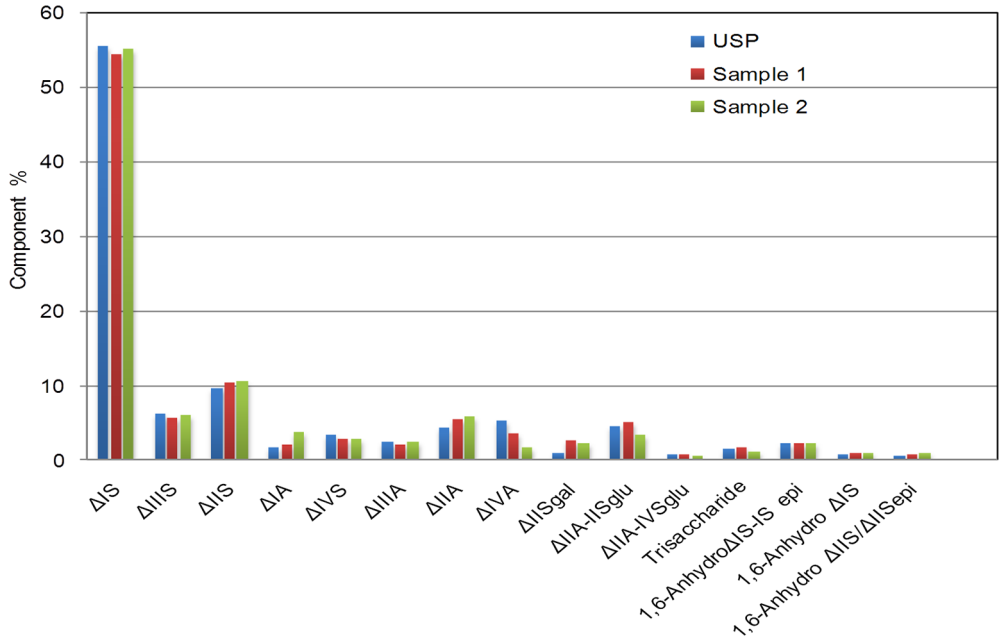

Figure 6. Comparison of the full composition of enoxaparin samples from three different lots. The chart was constructed using the average values (n = 3) from each enoxaparin sample. The ±SD values are given in Table S3 in the Suporting Information.

Table 2. Molar Percentage of Components Containing a 1,6-Anhydro Structure at the Reducing End

	% 1,6 anhydro	
sample	SAX	CZE
USP	21.4	21.3
sample 1	23.8	23.0
sample 2	21.3	20.1

The electrophoretic mobility of each oligosaccharide calculated with eq 1 is listed in Table 1. A good correlation (regression coefficient R^2 = 0.98) between the calculated and measured electrophoretic mobility for all oligosaccharides (except ΔIVA) was obtained (Figure 5b), indicating that this approach to peak assignment was reasonable. Thus, we were able to assign the peaks one by one based on electrophoretic mobility.

In addition to the theoretical prediction based on electrophoretic mobility, the identification of the four 1,6-anhydro oligosaccharide derivatives was further verified by comparing the electropherogram of the exhaustively digested enoxaparin with that of UFHs (Supporting Information, Figure S3). Because 1,6-anhydro derivatives were present only in enoxaparin, they were expected to correspond to the extra peaks (numbered 13−17 and 10) in the electropherogram of exhaustively digested enoxaparin. According to the calculated electrophoretic mobility, the four 1,6-anhydro oligosaccharides followed the migration order, from first to last: 1,6-anhydro ΔIS-IS, 1,6-anhydro ΔIS, and 1,6-anhydro ΔIIS/ΔIIS epi. From this information, peak 15 was identified as 1,6-anhydro ΔIS, while peaks 16 and 17 with identical peak areas were assigned as a pair of epimers of 1,6-anhydro ΔIIS/ΔIIS epi. However, the predicted electrophoretic mobility of 1,6-anhydro ΔIS-IS was only slightly higher than that of trisaccharide, making it difficult to distinguish these two peaks by electrophoretic mobility alone. However, we were able to distinguish them using a third strategy, i.e., by comparing their normalized peak areas with those determined with SAX-HPLC (Figure S4 in the Supporting Information).[45] Using this approach, peaks 11 and 13 were assigned as 1,6-anhydro ΔIS-IS and trisaccharide, respectively (Figure S3 in the Supporting Information). Peaks 9, 10, 11, and 12 were also identified by electrophoretic mobility.

The run-to-run and day-to-day repeatability in terms of migration times and peak areas of all the building blocks are listed in Table S3 in the Supporting Information. The average intraday (n = 6) and interday (n = 3) RSDs of migration times and peak areas were less than 0.9% and 2%, respectively, demonstrating the high precision of the method. The sensitivity and linearity of the method were evaluated using only standard disaccharide ΔIS, as all the building blocks had similar molar extinction coefficients of ∼5500 cm^{-1} M^{-1} at 232 nM.[24,46] The calibration curve for ΔIS was constructed by taking measurements of serial dilutions of the 1.46 mg/mL solution (Figure S5 in the Supporting Information). The linear regression analysis indicated a good correlation (R^2 = 0.998) between peak areas and concentration. The limit of detection was determined to be 0.023 mg/mL, and the limit of quantitation was determined to be 0.046 mg/mL.

The molar percentage of the components containing a 1,6-anhydro structure was calculated using the normalized area percentage according to the following formula:

$$\%\ \text{1,6-anhydro} = 100 \times \frac{\text{MW}}{\sum \text{MW}_x \times \text{area}_x} \times (\text{area}\Delta\text{IS1,6-anhydro} + \text{area}\Delta\text{IIS1,6-anhydro} + \text{area}\Delta\text{IISepi1,6-anhydro} + \text{area}\Delta\text{IS-IS1,6-anhydro}) \quad (2)$$

where MW is the mass-average molecular mass; MW_x and $area_x$ are the molecular weight and the area, respectively, of the peak x corresponding to the numbers listed in Table S1 in the Supporting Information; and areaΔIS1,6-anhydro, areaΔIIS1,6-anhydro, and areaΔIISepi1,6-anhydro and areaΔIS-IS1,6-anhydro correspond to the peak areas of 1,6-anhydro derivatives 15, 16, 17, and 14. The % 1,6-anhydro of enoxaparin from USP and two different manufacturers were evaluated

dx.doi.org/10.1021/ac303185w | Anal. Chem. XXXX, XXX, XXX−XXX

using our CE method. The % 1,6-anhydro values obtained by CZE were highly consistent with those obtained by SAX-HPLC (Table 2). The CZE method exhibited good repeatability (intraday RSD = 2%, n = 6) comparable with that of the SAX-HPLC method (RSD = 3%). However, we found that the SAX-column was easily contaminated by bovine serum albumin and heparinases present in the digestion buffer. Additionally, reduction of sample by sodium borohydride was needed to avoid peak splitting because of the presence of α/β anomers at the oligosaccharide reducing end.[45] In CE, the open tubular column eliminated the possibility of column contamination, and sample reduction was unnecessary because there is no significant difference in electrophoretic mobility between α and β anomers. Therefore, CZE is an attractive alternative to SAX-HPLC for the determination of % 1,6 anhydro derivatives.

A comparison of the enoxaparin composition among three sample lots is shown in Figure 6 (the calculation formula and data are given in Table S4 in Supporting Information). The weight percentages of the major building blocks (ΔIS, ΔIIS, and ΔIIIS) are very similar across all three lots of enoxaparin (% RSD 1−6%). There was relatively high variation in the weight percentages of 1,6-anhydro building blocks (% RSD 2−28%). For other minor disaccharides ΔIA, ΔIVA, and ΔIIS_{gal}, the weight percentages were rather variable (% RSD 40−53%, see Table S4 in the Supporting Information). These data were consistent with those obtained by SAX-HPLC.

CONCLUSIONS

In this study, structural analysis of enoxaparin was performed by combination of UPSEC/Q-TOF-MS with CZE. UPSEC/Q-TOF-MS enabled profiling of intact enoxaparin. On the basis of the obtained high resolution mass spectra, 70 components of enoxaparin were identified. Moreover, from the constructed EICs, the peak area ratios among the unsaturated, saturated, and 1,6-anhydro tetrasaccharides were measured. The changes in the components of therapeutic LMWHs in manufacturing processes can be rapidly scanned using this proposed method. All the building blocks of enoxaparin, especially for those oligosaccharides with the nearly same charge-to-mass ratio, can be baseline separated by addition of PEG10000 and $MgCl_2$ to the running buffer, demonstrating that CZE can be an effective tool for conducting a detailed compositional analysis of LMWHs. Compared with the SAX-HPLC method, the new CZE method is simpler, faster, and more cost-effective. Our approach can be potentially used to elucidate the contribution of each structural feature to the bioactivity of LMWHs.

ASSOCIATED CONTENT

Supporting Information

Additional information as noted in text. This material is available free of charge via the Internet at http://pubs.acs.org.

AUTHOR INFORMATION

Corresponding Author

*E-mail: jingwu.kang@sioc.ac.cn. Phone: 0086-21-54925385. Fax: 0086-21-54925481.

Notes

The authors declare no competing financial interest.

ACKNOWLEDGMENTS

We thank Dr. Weibin Chen for critically reading the manuscript. This work was financially supported by the National Natural Science Foundations of China (Grants 21175146, 20975109, and 90713021) and the Significant Innovation Project in New Drug Development from the Ministry of Science and Technology of China (Grant 2011ZX09202-101-10).

REFERENCES

(1) Linhardt, R. J.; Gunay, N. S. *Semin. Thromb. Hemost.* **1999**, *25*, 5−16.
(2) Weitz, J. I. *New Engl. J. Med.* **1997**, *337*, 688−699.
(3) Mousa, S. A.; Mohamed, S. *Oncol. Rep.* **2004**, *12*, 683−688.
(4) Lewis, E. J.; Xu, X. *Diabetes Care* **2008**, *31*, S202−S207.
(5) Sain, M.; Kovacic, V.; Radic, J.; Ljutic, D.; Jelicic, I. *Drugs Aging* **2012**, *29*, 1−7.
(6) Fareed, J.; Iqbal, O.; Nader, H.; Mousa, S.; Wahi, R.; Coyne, E.; Bick, R. L. *Clin. Appl. Thromb. Hemost.* **2005**, *11*, 363−366.
(7) Casu, B. *Adv. Carbohydr. Chem. Biochem.* **1985**, *43*, 51−134.
(8) Casu, B.; Lindahl, U. *Adv. Carbohydr. Chem. Biochem.* **2001**, *57*, 159−206.
(9) Ruiz-Calero, V.; Puignou, L.; Galceran, M. T. *J. Chromatogr., A* **1998**, *828*, 497−508.
(10) Jones, C. J.; Beni, S.; Limtiaco, J. F. K.; Langeslay, D. J.; Larive, C. K. *Annu. Rev. Anal. Chem.* **2011**, *4*, 439−465.
(11) Fareed, J.; Leong, W. L.; Hoppensteadt, D. A.; Jeske, W. P.; Walenga, J.; Wahi, R.; Bick, R. L. *Semin. Thromb. Hemost.* **2004**, *30*, 703−713.
(12) Lima, M. A.; de Farias, E. H. C.; Rudd, T. R.; Ebner, L. F.; Gesteira, T. F.; Mendes, A.; Bouças, R. I.; Martins, J. R. M.; Hoppensteadt, D.; Fareed, J.; Yates, E. A.; Sassaki, G. L.; Tersariol, I. L. S.; Nader, H. B. *Carbohydr. Polym.* **2011**, *85*, 903−909.
(13) Guerrini, M.; Elli, S.; Gaudesi, D.; Torri, G.; Casu, B.; Mourier, P.; Herman, F.; Boudier, C.; Lorenz, M.; Viskov, C. *J. Med. Chem.* **2010**, *53*, 8030−8040.
(14) Adiguzel, C.; Jeske, W. P.; Hoppensteadt, D.; Walenga, J. M.; Bansal, V.; Fareed, J. *Clin. App. Thromb. Hemost.* **2009**, *15*, 137−144.
(15) Mao, W.; Thanawiroon, C.; Linhardt, R. J. *Biomed. Chromatogr.* **2002**, *16*, 77−94.
(16) Lohse, D. L.; Linhardt, R. J. *J. Biol. Chem.* **1992**, *267*, 24347−24355.
(17) Imanari, T.; Toida, T.; Koshiishi, I.; Toyoda, H. *J. Chromatogr., A* **1996**, *720*, 275−293.
(18) Koketsu, M.; Linhardt, R. J. *Anal. Biochem.* **2000**, *283*, 136−145.
(19) Pervin, A.; Alhakim, A.; Linhardt, R. J. *Anal. Biochem.* **1994**, *221*, 182−188.
(20) Duteil, S.; Gareil, P.; Girault, S.; Mallet, A.; Feve, C.; Siret, L. *Rapid Commun. Mass Spectrom.* **1999**, *13*, 1889−1898.
(21) Korir, A. K.; Limtiaco, J. F. K.; Gutierrez, S. M.; Larive, C. K. *Anal. Chem.* **2008**, *80*, 1297−1306.
(22) Galeotti, F.; Volpi, N. *Anal. Chem.* **2011**, *83*, 6770−6777.
(23) Yang, B.; Weyers, A.; Baik, J. Y.; Sterner, E.; Sharfstein, S.; Mousa, S. A.; Zhang, F.; Dordick, J. S.; Linhardt, R. J. *Anal. Biochem.* **2011**, *415*, 59−66.
(24) Brustkern, A. M.; Buhse, L. F.; Nasr, M.; Al-Hakim, A.; Keire, D. A. *Anal. Chem.* **2010**, *82*, 9865−9870.
(25) Wang, B.; Buhse, L. F.; Al-Hakim, A.; Ii, M. T. B.; Keire, D. A. *J. Pharm. Biomed. Anal.* **2012**, *67−68*, 42−50.
(26) Mourier, P. A. J.; Viskov, C. *Anal. Biochem.* **2004**, *332*, 299−313.
(27) Jones, C. J.; Beni, S.; Limtiaco, J. F. K.; Langeslay, D. J.; Larive, C. K. *Annu. Rev. Anal. Chem.* **2011**, *4*, 439−465.
(28) Seo, Y.; Andaya, A.; Leary, J. A. *Anal. Chem.* **2012**, *84*, 2416−2423.
(29) Saad, O. M.; Ebel, H.; Uchimura, K.; Rosen, S. D.; Bertozzi, C. R.; Leary, J. A. *Glycobiology* **2005**, *15*, 818−826.
(30) Saad, O. M.; Leary, J. A. *Anal. Chem.* **2003**, *75*, 2985−2995.
(31) Saad, O. M.; Leary, J. A. *Anal. Chem.* **2005**, *77*, 5902−5911.
(32) Zaia, J. *Mass Spectrom. Rev.* **2004**, *23*, 161−227.
(33) Zaia, J. *Mass Spectrom. Rev.* **2009**, *28*, 254−272.

(34) Thanawiroon, C.; Rice, K. G.; Toida, T.; Linhardt, R. J. *J. Biol. Chem.* **2004**, *279*, 2608−2615.
(35) Doneanu, C. E.; Chen, W.; Gebler, J. C. *Anal. Chem.* **2009**, *81*, 3485−3499.
(36) Staples, G. O.; Bowman, M. J.; Costello, C. E.; Hitchcock, A. M.; Lau, J. M.; Leymarie, N.; Miller, C.; Naimy, H.; Shi, X.; Zaia, J. *Proteomics* **2009**, *9*, 686−695.
(37) Li, L.; Zhang, F.; Zaia, J.; Linhardt, R. J. *Anal. Chem.* **2012**, *84*, 8822−8829.
(38) Zaia, J.; Costello, C. E. *Anal. Chem.* **2001**, *73*, 233−239.
(39) Henriksen, J.; Ringborg, L. H.; Roepstorrf, P. *J. Mass Spectrom.* **2004**, *39*, 1305−1312.
(40) Ziegler, A.; Zaia, J. *J. Chromatogr., B* **2006**, *837*, 76−86.
(41) Eldridge, S. L.; Higgins, L. A.; Dickey, B. J.; Larive, C. K. *Anal. Chem.* **2009**, *81*, 7406−7415.
(42) Damm, J. B. L.; Overklift, G. T.; Vermeulen, B. W. M.; Fluitsma, C. F.; Dedem, G. W. K. v. *J. Chromatogr., A* **1992**, *608*, 297−309.
(43) Mosher, R. A.; Dewey, D.; Thormann, W.; Saville, D. A.; Bier, M. *Anal. Chem.* **1989**, *61*, 362−366.
(44) Casu, B.; Gennaro, U. *Carbohydr. Res.* **1975**, *39*, 168−176.
(45) Mourier, P.; ; .Viskov, C. *Method for determining specific groups constituting heparins or low molecular weight heparins*. U.S. Patent Application 2005/0119477 A1, June 2, 2005.
(46) Linker, A.; Hovingh, P. *Biochemistry* **1972**, *11*, 563−568.